pH-Switchable Unusual Electrical Conductance of a New Tripeptide-Gold-Nanoconjugate

Ray Sudipta[1], Dutta Dibakar[2] and Maiti Dilip K.[1*]
1. Department of Chemistry, University of Calcutta, INDIA
2. Department of Physics, St. Xavier's College, Kolkata, INDIA
*dkmchem@caluniv.ac.in

Abstract

We introduced a simple method for in situ preparation of stable gold nanoparticles by using a solution of a new tripeptide and $HAuCl_4$ without addition of any external reducing agent and developed the unique electrical properties of the nanoconjugate. In this regard, we have synthesized and characterized new WVY-tripeptide bearing Trp-, Val- and Tyr-residues. Structure of the designed tripeptide and self-assembly was calculated with DFT study.

Characterization and properties of the peptide-Au-nanoconjugate were investigated using UV-Vis, fluorescence, FT-IR, XRD, CD and TEM techniques. Tripeptide-Au-nanoconjugate solutions were studied for the I-V characteristics and unprecedented pH-switchable semiconducting and conducting properties were established with the nanomaterials.

Keywords: Peptides, Nanoparticle, I-V characterization, Peptide-Au-nanoconjugate.

Introduction

Recent progress in nanotechnology has shown highly promising capabilities of nanoparticles (NP) to function as powerful device for electronic and optical sensor application [1-4]. On the other hand self-assembly is one of the powerful strategies for nanofabrication[5-10] to achieve valuable nanomaterials,[11,12] which can be used in designing biological sensory labels,[13,14] electronic and optical devices,[15-17] bio-analytical tools[18,19] and catalysts.[20-23] Ordered network structure[24,25] may be achieved through conjugation of metal-NPs to the non-conducting-peptides, which may install innovative electronic transport property.

Development of this type synthetic metals[26-30] possessing innovative ionic, semiconducting, conducting and sensor properties was attractive because of their smaller weight, greater workability, corrosion resistance ability and lower cost. Conventional syntheses of colloidal metal-NPs are performed through borohydride/citrate reduction of metal salts followed by ligand exchange with suitable molecules bearing free –SH and/or -NH_2 group as stabilizer(s).[31]

Major disadvantage of these processes is that there is always possibility of aggregation among the NPs during the ligand exchange leading to formation of undesired larger particles. Mild reducing property of tyrosine[32,33] and tryptophan[34] may be employed as part of a short peptide for making self-assembly towards fabrication of metal-NPs as well as peptide-nanoconjugate without addition of traditional reducing agents.

The strategy to metal-NPs at ambient temperature using a small peptide is desirable because of its synthetic simplicity, compatibility with various biological systems and innovative application. Previously some works related to pH mediated self-assembly of peptide-gold or silver nanoparticle conjugate have been reported.[35,36]

However, small peptide-based gold nanoconjugates and their self-assembly in different pH medium with electrical insight have not been reported. Herein we demonstrate the new findings towards design, synthesis, self-assembly of a new tripeptide, their pH-programmable nanofabrication, characterization of peptide-Au-nanoconjugates and their valuable electrical conductance property.

Material and Methods

All reagents were purchased from commercial suppliers and used without further purification, unless otherwise specified. Commercially supplied ethyl acetate and petroleum ether were distilled before use. Petroleum ether used in our experiments was in the boiling range of 60°-80° C. L-tryptophan, L-Tyrosine, L-Valine, dicyclohexylcarbo-diimide (DCC), $AuCl_3$ and 1-hydroxy benzotriazole (HOBt) were purchased from SRL, India. Reagent grade HCl and NaOH were purchased from Merck, India, they were used to adjust the pH of the solution and for preparing the solution, HPLC grade distilled water has been used. Column chromatography was performed on silica gel (60-120 mesh, 0.120 mm-0.250 mm). Analytical thin layer chromatography was performed on 0.25 mm extra hard silica gel plates with UV254 fluorescent indicator.

Reported melting points are uncorrected. ^{1}H NMR and ^{13}C NMR spectra were recorded at ambient temperature using 300 MHz spectrometers (300 MHz for ^{1}H and 75 MHz for ^{13}C). Chemical shift is reported in ppm from internal reference tetramethylsilane and coupling constant in Hz. Proton multiplicities are represented as s (singlet), d (doublet), dd (double doublet), t (triplet), q (quartet) and m (multiplet). Infrared spectra were recorded on FT-IR spectrometer in thin film. HR-MS data were acquired by electron spray ionization technique on a Q-tof-micro quadruple mass spectrophotometer. Optical rotation of the chiral compounds was measured in a polarimeter using standard 10 cm quartz cell in sodium-D lamp at ambient temperature.

Synthesis of tripeptide 1: The tripeptide 1 employed in this report has been synthesized by the conventional solution phase methodology. The boc group was used for N-terminal protection and the C-terminus was protected as a methyl ester. Couplings were mediated using dicyclohexylcarbo-diimide and 1-hydroxybenzotriazole (DCC/HOBt). The final compounds were fully characterized by FT-IR ,^{1}H NMR and mass spectrometry (available at ESI).

Boc-Trp-OH (1): A solution of tryptophan (4.08 g, 20 mmol), dioxan (40 mL), water (20 mL) and aqueous NaOH (1M, 20 mL) was stirred and cooled in an ice-water bath. Di-*tert*-butylpyrocarbonate (4.4 g, 22 mmol) was added and stirring was continued at room temperature for 6 h.

The solution was concentrated in a rotary evaporater under reduced pressure at ambient temperature to the approximate volume 20 mL which was cooled in an ice-water bath, covered with a layer of ethyl-acetate (30 mL) and acidified with a dilute solution of $KHSO_4$ to pH 2.5 (Congo red). The aqueous phase was extracted with ethyl acetate and this operation was done repeatedly.

The ethyl acetate extracts were pooled, washed with water and dried over anhydrous Na_2SO_4 and evaporated under reduced pressure at ambient temperature. The pure material 1 was obtained. Yield = 4.86 g (16 mmol, 80%). ^{1}H NMR (300 MHz, $CDCl_3$)δ 8.09 (1H, s); 7.62-7.64 and 7.32-7.30 (2H, d, J = 6Hz); 7.23-7.09 (3H, m); 6.21-6.18 (1H, d, J = 9Hz); 4.40-4.38 (1H, m); 3.31-3.28 (2H, m); 1.44 (Boc-CH_3s, 9H, s). HR-MS (m/z) for $C_{16}H_{20}N_2O_4$: Calculated 304.1423, found 305.1457.

Boc-Trp-Val-OMe (2): Boc-Trp-OH (4.56 g, 15 mmol) was dissolved in a mixture of dichloromethane (DCM, 10 mL) in an ice-water bath. H-Val-OMe was isolated from corresponding methyl ester hydrochloride (5.01 g, 30 mmol) by neutralization, subsequent extraction with ethyl acetate and concentration to 10 mL and this was added to the reaction mixture followed immediately by 3.09 g (15 mmol) of di-cyclohexaylcarbo-diimide (DCC).

The reaction mixture was allowed to come to room temperature and stirred for 24 hrs. DCM was evaporated, residue was taken in ethyl acetate (60 mL) and dicyclohexylurea (DCU) was filtered off.

The organic layer was washed with HCl (2M, 3 × 50 mL), brine (2 × 50 mL), sodium carbonate (1M, 3 × 50 mL) and brine (2 × 50 mL) respectively, then dried over anhydrous sodium sulfate and evaporated in vacuo to yield 2 as a solid sample. Yield = 80% (5.0 g, 12 mmol). ^{1}H NMR (300 MHz , $CDCl_3$) δ 8.12 (1H, s); 7.67-7.65 and 7.37-7.34 (2H, d, J = 6Hz and J = 9Hz); 7.23-7.09 (3H, m); 6.31-6.28 (1H, d, J = 9Hz); 5.17 (1H, b); 4.42-4.38 (1H, m); 4.13-4.08 (1H, m); 3.63 (3H, s); 3.33-3.26 (2H, m); 3.22-3.15 (1H, m); 1.46 (9H, s); 0.81-0.76 (6H, m). HR-MS (m/z) for $C_{22}H_{33}N_3O_5$: Calculated 431.2420, found 432.2454.

Boc-Trp-Val-OH (3): Boc-Trp-Val-OMe (4.6 g, 11 mmol) was taken in MeOH (20 mL) and NaOH (2M, 10 mL) was added. The reaction mixture was stirred and the progress of saponification was monitored by thin layer chromatography (TLC). After 10 h methanol was removed under *vacuo*, the residue was taken in 50 mL of water, washed with diethyl ether (2 × 50 mL). Then the pH of the aqueous layer was adjusted to 2 using drop wise addition of HCl (1M) and it was extracted with ethyl acetate (3 × 50 mL). The extracts were pooled, dried over anhydrous sodium sulfate and evaporated *in vacuo* to yield 3 as a solid compound.

Yield = 3.5 g (8.68 mmol, 79%). ^{1}H NMR (300 MHz , DMSO-d_6) δ 8.36 (1H, s); 7.67-7.65 and 7.35-7.33 (2H, d, J = 6Hz); 7.20-7.02 (3H, m); 6.33-6.31 (d, J = 9Hz); 5.28 (1H, b); 4.37-4.33 (1H, m); 4.15-4.08 (1H, m); 3.31-3.25 (2H, m); 3.22-3.14 (1H, m); 1.43 (9H, s); 0.86-0.80 (6H, m). HR-MS (m/z) for $C_{22}H_{31}N_3O_5$: Calculated 417.2264, found 418.2297.

Boc-Trp-Val-Tyr-OMe (4): Boc-Trp-Val-OH (2.01 g, 5 mmol) was taken in DMF (10 mL) and the solution was cooled in an ice-water bath. Then H-Tyr-OMe (2.31 g, 10 mmol) was isolated from the corresponding methyl ester hydrochloride by neutralization, subsequent extraction with ethyl acetate and concentration to 10 mL. It was then added to the reaction mixture followed immediately by the addition of DCC (1.03 g, 5 mmol) and HOBt (0.675 g, 5mmol). The reaction mixture was stirred for three days. The residue was taken in ethyl acetate (60 mL) and the DCU was filtered off. The organic layer was washed with HCl (2M, 3 × 50 mL), brine (2 × 50 mL), sodium carbonate (1M, 3 × 50 mL) and brine (2 × 50 mL) respectively. Then dried over anhydrous sodium sulfate was evaporated in vacuo to yield peptide 1 (4) as an white solid. Purification was done by silica gel column (100-200mesh) using 3:1 ethyl acetate - toluene as eluent.

Yield =80% (2.23 g, 4 mmol,). ^{1}H NMR (300 MHz , $CDCl_3$) δ9.80(1H, s); 7.66-7.63 (1H, d, *J* = 9 Hz), 7.56 (1H, s), 7.55-7.37 (2H, d, *J* = 4 Hz) 7.17-6.99 (6H, m); 6.79-6.77, (2H, d, *J* = 6Hz); 5.74 (1H, m); 4.68-4.66 (1H, m); 4.43 (1H, m) 4.31-4.26 (1H, m); 3.69 (3H, s); 3.28-3.18 (2H, m); 2.63-2.61 (1H, m); 2.20-2.19 (1H, m); 2.09-2.02 (1H, m); 1.42 (9H, s); 0.89-0.81 (6H, m). ^{13}C NMR (75 MHz, $CDCl_3$) δ171.3, 171.2, 170.2, 155.6, 135.7, 129.5,126.2, 122.9, 120.8, 118.2, 118.0, 115.0, 110.7, 109.4, 77.6, 57.5, 53.1, 51.3, 36.0, 30.3, 27.6, 18.4, 17.1. HR-MS (*m/z)* for $C_{32}H_{48}N_4O_7$: Calculated 600.3050, found 602.7460. FT-IR Data (KBr, cm^{-1}) 3545, 3290, 2220, 2190, 2080, 1966,1763, 1656,1594, 1430.

Formation of Peptide-Au-Nanoconjugate: To a peptide solution (5mL, 50 mM) in MeOH, 5ml of aqueous solution of $HAuCl_4$ (10 mM) was added. Then the pH of the solution was adjusted to 11 with NaOH (1 M) solution. This solution after the formation of the nanoparticle was made acidic by using a standard HCl solution. The pH of the 1:1 methanol-

water solution containing peptide-Au-NPs nanoconjugate gradually decreases by dropwise addition of HCl. Finally, TEM of the sample was taken 15 min after the adjustment of the pH of the medium.

DFT study for energy minimization of peptide 1: Our entire calculations were performed at HF and DFT/B3LYP using Gaussian 09 program package, invoking gradient geometry optimization. The geometry of the investigated compound in the ground state is fully optimized. First we performed the geometrical optimization of the molecules using the DFT method with B3LYP and 6-31G basis set. We achieved the stabilizing energy as -1223.9538 × 10^3 Kcal/mol. Among the numerous available DFT methods, we have selected the B3-LYP method which combines the Becke's three parameter exchange functional (B3) with the Lee, Young and Parr correlation functional (LYP). All the calculations are performed by using GaussView 5.0.8 molecular visualization program Package.

The computational study for the optimized molecular structural parameters and HOMO – LUMO energy gap for peptide 1 have been investigated using B3LYP/6-311G basis set and it has been observed as 0.41 eV. Our calculated results have shown that the investigated compound possesses a dipole moment of 1.7527 Debye by using HF calculation with a 6-31G basis set. We achieved the stabilizing energy as -1216.3102 × 10^3 Kcal/mol. The energy minimized molecular structure of peptide 1 shows a turn due to the presence of intermolecular hydrogen bond (2.5 Å) and CH-π interaction (3.8 Å).

From higher order packing along *b*- axis, it has been observed that π- π interaction is present which helps to form a sheet like structure upon self-assembly. Our entire calculations were performed at HF and DFT/B3LYP using Gaussian 09 program package, invoking gradient geometry optimization. All the calculations are performed by using GaussView 5.0.8 molecular visualization program Package. DFT study enabled us to find out the Boc-Trp-Val-Tyr-OMe (4) or tripeptide 1 with nanospace (figure 1 Bb) for generation of Au-NPs to achieve peptide-Au-nanoconjugates.

Results and Discussion

In a continuous effort for computational study[37-40], we have designed a new small peptide 1 (Boc-Trp-Val-Tyr-OMe, figure 1 Aa) with HOMO-LUMO energy gap 0.41 eV (acceptor) using DFT optimization (figure 1B,c) as implemented in Gaussian 09 [41].The Trp- and Tyr-residues possessing mild reducing property were placed adjacent to each other which were separated by Val residue. Hence it is capable of structural change in demand especially during creation of space (figure 1 Bb) for fabricating small Au-NPs. The DFT investigation confirmed the strong self-assembly nature of the peptide through π-π stacking and other noncovalent binding forces (figure 1 Bd), which is important for making innovative synthetic materials.

The peptide WVY was obtained through four step solution phase synthesis using boc group protected N-terminal and methyl ester bearing C-terminus. The N-C couplings were achieved using dicyclohexylcarbodiimide (DCC) and 1-hydroxybenzotriazole (HOBT). In our experiments, generation of Au-NPs was noticed visually with change of pH of the peptide 1 solution (figure 1C) containing $HAuCl_4$. Existence of fabricated Au-NPs was confirmed through recording UV-Vis spectra of the samples (figure 2A). From figure 1C, it was observed that at pH~6, closer to the isoelectric point (6.08), the color of the peptide-Au-NPs-conjugate suspension is pink. Lowering of pH through addition of aqueous HCl (1N), the color of the peptide-Au-nanoconjugate solution changed from violet (pH = 4) to deep blue (pH = 2).

On the other hand, by increase of pH through addition of an aqueous NaOH (1N), the color of the peptide-Au-NPs darkened from pink to red (pH = 10) and subsequently deep wine-red at pH 12. The colorimetric data are in accordance with the observed UV-Vis spectra of the Au-NPs- tripeptide solution (figure 2A).

UV-Vis band appears at 535nm at pH~6 and it was red shifted on decreasing the pH values of the solution with color change in the peptide-Au-NPs suspension from pink to blue. The peptide-Au-NPs conjugate revealed UV-Vis band in the range of 535-527nm due to nanofabrication of the small Au-NPs ranging 5-20nm. Next we turned our attention for HR-TEM imaging of the pure peptide solutions at pH~6 showing formation of vesicle-like self-assembled system whereas both fibriller and vesicle-like structure were observed at pH~9 (figure S1a-d, available at ESI). The peptide-Au-nanoconjugates were well dispersed at pH 11 and the Au-NPs are having spherical morphology (figure 2B c) of average diameter 4-5nm (figure 2B e).

The Au-NPs were well dispersed in solution at pH 8 and 9 with growth (8-12nm) and slightly change in the shape given in supporting figure S2 (a) and (b) (available at ESI). At the all basic pH, peptide 1 was used as a template showing no specific morphology, but at pH~6 the sole peptide solution formed vesicle-like morphology and the Au-NPs were templated on these vesicles (figure S3a-d available at ESI). At this pH, formation of peptide-Au-NPs-conjugates was observed from HR-TEM images and the size of the Au-NPs was changing at higher pH 4-5nm and at lower pH 8-12nm. The main aspect is that change in particle-particle distance occurred upon altering the pH of the solution which is due to the self-assembly process of peptide 1.

From the above TEM pictures we can conclude that the assembly process is more controlled around the neutral pH compared to that of both lower and higher pH. FT-IR study was carried out to understand the exact nature of the interactions involved between the Trp- and Tyr-residues of peptide 1 and Au-NPs. The conjugation of the peptides with

the Au-NPs was confirmed from the FTIR study of the peptide-Au-NPs-conjugates.

FTIR spectra recorded of peptide-1 given in supporting figure S4 (available at ESI) and peptide-Au-nanoconjugate displayed peaks at 3545cm^{-1} and 1594cm^{-1} which may be attributed due to the Trp-Indolic-NH and amide-NH stretching and bending vibration respectively. The ester carbonyl vibration band appeared at1763cm^{-1}. The first peak was completely broadened appearing at 3408cm^{-1} for peptide-Au-nanoconjugate indicating peptide binding with the gold surface *via* Au-N bond formation mainly with indole-NH part and the absence of the peak about 1763cm^{-1} due to the carbonyl ester moiety which indicates its hydrolysis under the experimental conditions.

The spectrum of peptide-Au-NPs displayed two prominent band at 1652 and 1595cm^{-1} corresponding to the band produced by amide I and amide II of the peptide-1. The position and nature of the amide bands in peptide-Au-NPs-conjugates were not same as those of the pure peptide-1.

To establish the role of conformational change for stabilizing Au-NPs, CD structural study was performed under acidic (pH~2) and basic (pH ~11) conditions (figure 3 A). For meaningful comparison, the CD spectrum at neutral pH is also performed in 1:1 methanol-water solution. It is observed from the CD-spectral study that the peptide-1 adopts beta sheet conformation in 1:1 methanol-water solution at neutral pH. But upon conjugation with Au-NPs, a conformational change is observed which might be due to adoption of some kind of turn structure of the peptide molecule for stabilizing the Au-NPs.

In contrary to very little effect of pH upon conformational change of peptide 1 with NPs in solution, herein CD structural analysis revealed severe conformational change of the tripeptide molecule upon conjugation with Au-NPs. Fluorescence spectroscopic measurements were carried out to investigate the mechanism of reduction by the tryptophan and tyrosine residue of the peptide in the process of formation of Au-NPs-peptide-conjugate (figure 3B).

The peptide 1 solution upon excitation at 270 nm emitted at 375 nm (figure 8e) which is a characteristic peak for tryptophan residue whereas peptide-Au-nanoconjugate solution did not reveal any emission peak at this position. Interestingly on excitation of this solution at 320nm, an emission peak appeared at 395nm. It indicates that some part of the peptide residue dimerizes upon the pH responsive Au-composite formation to the corresponding di-tryptophan moiety which emitted at 395nm and observed for pH 10, 8 and 6. Upon changing the pH of the solution at 2, there was a slight shift in the peak position to 410nm.

The peptide-Au-NPs composite formation is also supported by XRD study (figure S5 available at ESI). From the XRD patterns of the solid peptide-1, peptide 1 in 1:1 methanol-water solution and peptide-Au-nanocomposite observed that there was no peak or hump for solid peptide and peptide 1 in solution. One hump arises at $2\theta = 38^{O}$ which corresponds to 111 plane for Au-NPs. Another peak appears at $2\theta = 45^{O}$ which corresponds to 200 plane of the Au-NPs.

There has been a lot of interest in self-organisation of metal nanoparticles and in electronic transport through the ordered network structures.[42] In general, three dimensional network of peptide-nanoparticle conjugate can readily be obtained depending on the functionality and the inter-particle spacing, hence interesting electrical properties are expected From the characteristic *I-V* plotting (figure 4 A), it has been found that the conductance of the only peptide solution at pH 6 is negligible in amount i.e. the peptide moiety at this pH range is almost nonconducting in nature.

Though we all know that the metallic gold is a very good conductor of electricity, but the electrical conductance of gold nanoparticles is drastically different from bulk metallic gold. Depending upon their particle size, shape and their external condition, the electrical behaviour of gold-nanoparticles is of two types, it might be high conducting e.g. metallic in nature and another is that it has a medium conductance nature.

In the current-voltage plotting we found two observations: one is the peptide-Au-nanocomposite solution at pH 2 shows some conducting nature with respect to the non-conducting peptide solution. This increase in conductance value might be due to the presence of gold nanoparticles in the solution. Another is that the peptide-Au-nano conjugate solution at pH 11 shows much higher conductance with respect to the peptide-Au-nano conjugate solution at pH 2. This increase in conductance might be due to the greater number of freely moveable small particle size gold nanoparticles and their specific alignment with ionic peptide solution during this experiment which might not be possible for the peptide-Au-nanocomposite at pH 2 because mostly all nanoparticles self-assemble to form gold nano cluster which has been observed from the TEM experiment at this pH range.

The variation of conductivity is observed for peptide-Au-nanocomposite at pH 11 over a frequency range from 500 kHz to 2MHz for different temperatures (figure 4B). From the graph it is noticed that for any particular frequency over the frequency range, the conductivity of the sample shows an increasing trend with the rise in temperature. This kind of behaviour is the characteristics of semiconducting and ionic materials. Also, it can be seen from the graph that for any particular temperature, the conductivity of the sample showed a sharp rise with the rise in frequency, thereby exhibiting a frequency dispersion of conductivity.

Herein, we have synthesized the tripeptide WVY and its Au-nanoconjugate. The different characterization data indicate that the self-assembling nature of peptide 1 and peptide-Au-nanoconjugate might be very different, It seems that not only

the metal conjugation but also the pH of the medium also has immense influence in the self-assembly. From DFT calculation it was observed the there was a considerable electron density over Tryptophan residue as well as creation of nano space can be possible upon self-assembly of peptide 1.

The tyrosine and tryptophan residue both can behave as reducing agent here and the Au-nanoparticle formed can be arranged inside the nano space. From the FT-IR study, it has been observed that the position and nature of the amide bands in the peptide-1-AuNP conjugates are not same as those of the neat peptide-1 which indicates the peptide-1 adopted some conformational change on binding with the Au-NPs. surface. CD study as well as fluorescence spectroscopic measurements also suggest the peptide-1-AuNP conjugates might adopt some type of conformational change upon binding with the Au-nanoparticle.

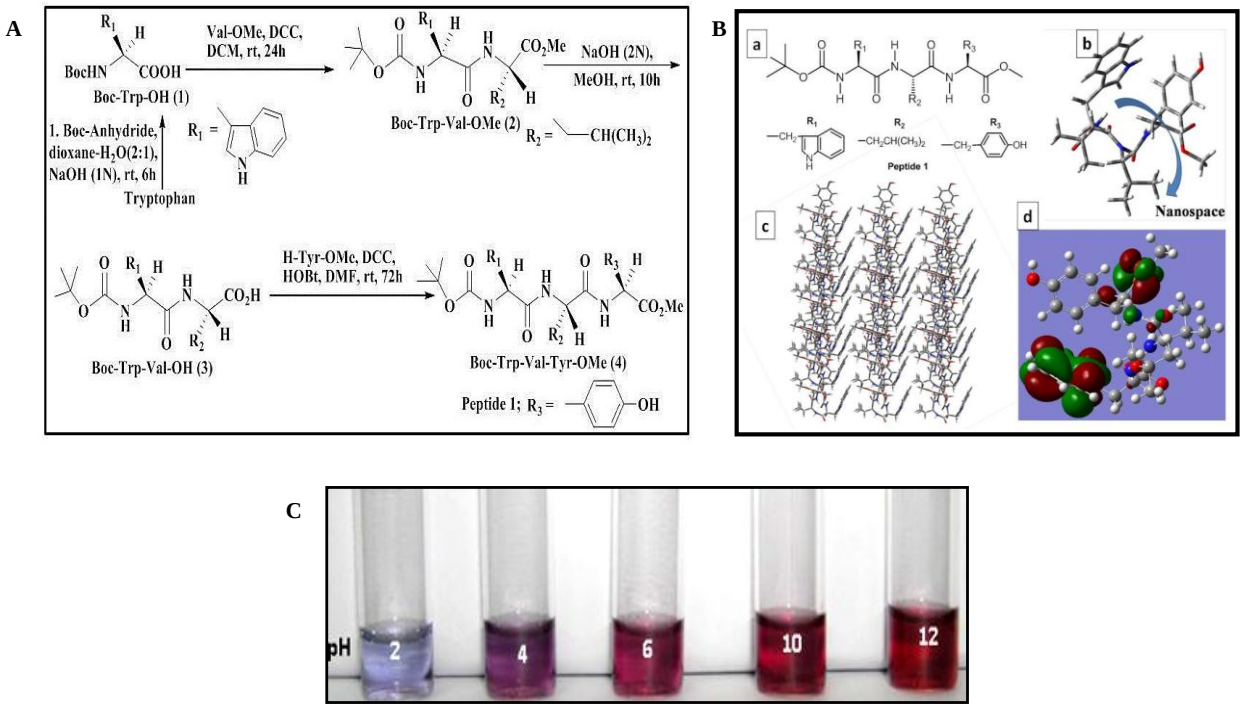

Figure 1: A: Schematic representation of the synthesis of tripeptide Boc-Trp-Val-Tyr-OMe. B: (a) Peptide 1 WVY; (b) creation of nano space; (c) DFT-B3LYP/6-311G calculated HOMO-LUMO; (d) Highly ordered self-assembly diagram along *b*-axis with strong intermolecular *π*-*π* stacking. C: Peptide-1-Au-NPs conjugate solution at pH ranging from 2 to 12

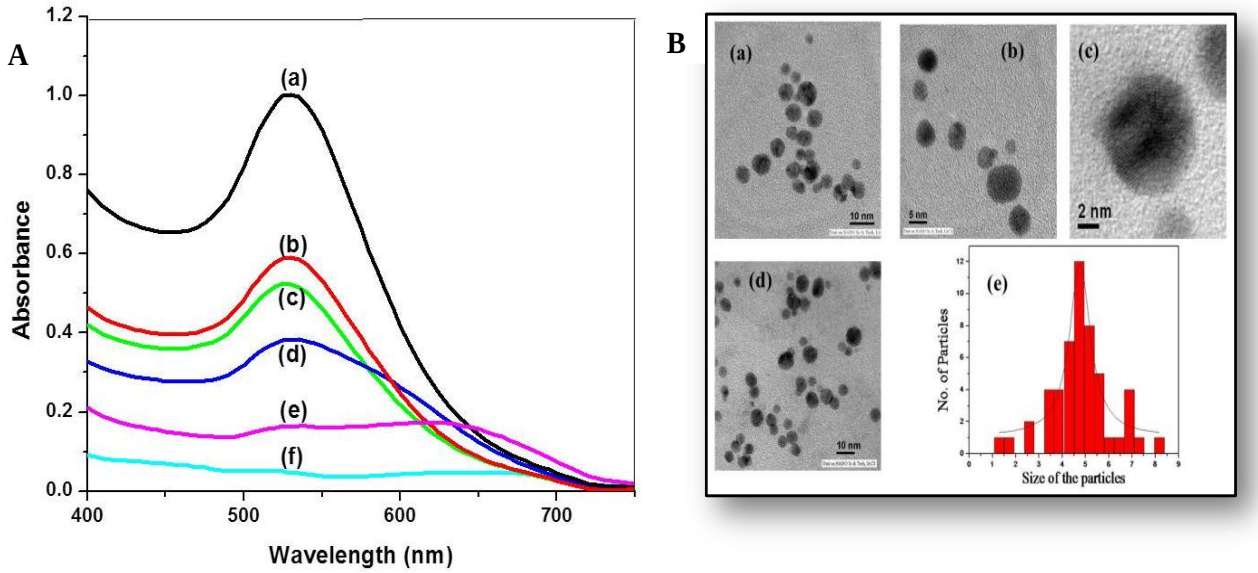

Figure 2: A: UV-Vis absorbance spectra of peptide-Au-NPs in solutions at different pH values (a-pH 12, b-pH 10, c-pH 8, d-pH 6, e-pH 4, f-pH 2) showing respective plasmon band for peptide-Au-nanoconjugate. B: (a-d) HR-TEM Images of peptide-Au-NPs at pH 11; (e) histogram of Au-NPs.

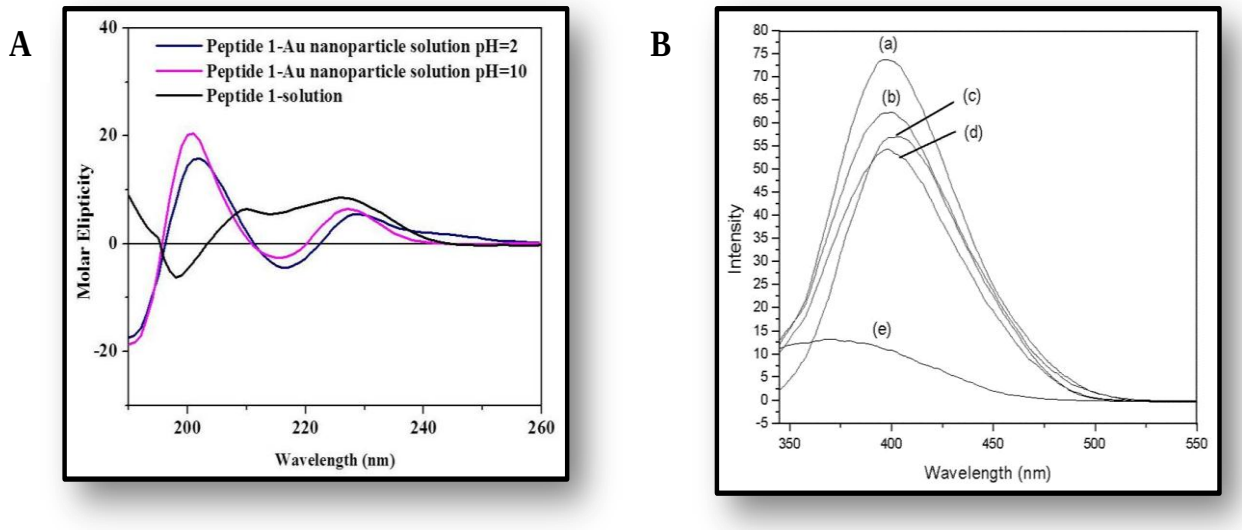

Figure 3: A: CD spectra of peptide and peptide-Au-NPs at different pH of the solutions, B: Emission spectra of peptide-AuNPs solution at different pH values from (a) to (d). Whereas (e) represents the emission spectrum of peptide 1 with an excitation value from 280 nm.

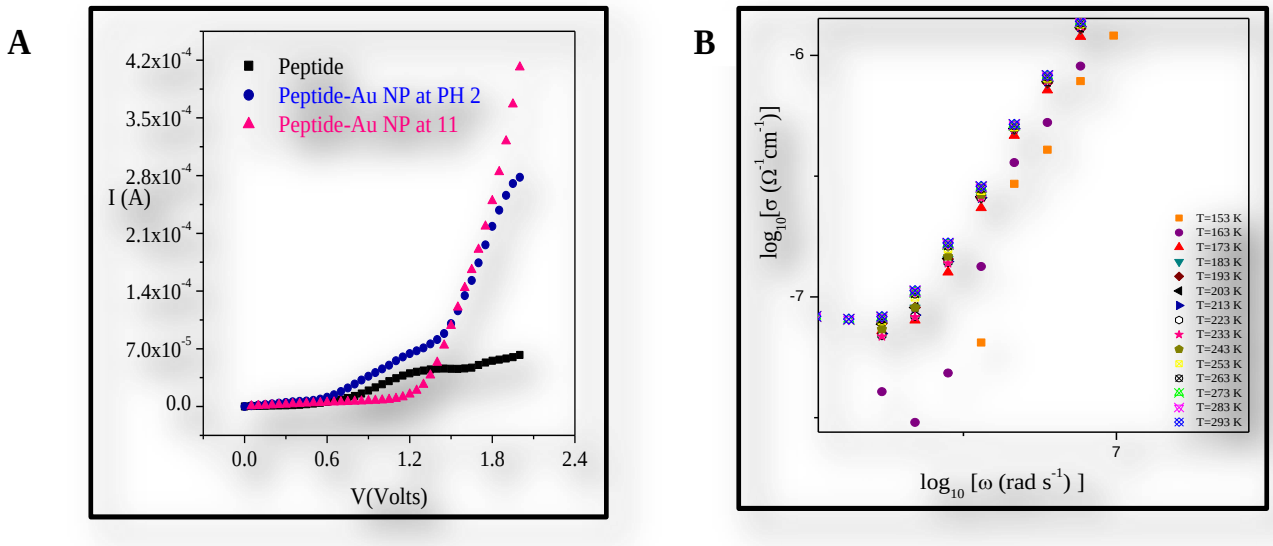

Figure 4: A: Characteristic *I-V* plotting of peptide solution, peptide-Au-NPs solution at pH 2 and 11, B: Variation of conductivity for peptide-Au-NPs at pH 11 over a frequency range from 500 kHz to 2 MHz at different temperatures.

These differences in their conformational arrangement also reflect their different behavior in characteristic *I-V* plotting. The neat peptide shows non-conducting behavior whereas the peptide-Au-nanoconjugate shows some conductance. Also, the switchable increase of conductance of the peptide-Au-nanocomposites through simple alteration of pH is significant for designing and fabrication of valuable nano-devices and developing innovative biological sensors.

Conclusion

In conclusion we have successfully designed and synthesized a new small tripeptide WVY possessing specific sequencing which was exploited as a reducing agent as well as template for size and shape tunable nanofabrication and stabilization of small Au-NPs with change in pH of the solution containing $HAuCl_4$. FT-IR, CD, photo-physical and XRD studies were performed to understand the specific role of the small peptide as synthetic materials and mechanism of pH-dependent nanofabrication.

The peptide-Au-nanoconjugate solution at different pH displayed conducting nature. We believe that these results could pave the way to design and synthesis of small new peptides/polymers, pH-programmable fabrication of small metal-NPs and smart peptide-metal-nanoconjugates and their innovative properties, which have considerable impact in the futuristic application as nano biosensors and nanodevices.

Acknowledgement

SR is thankful to UGC, New Delhi for DSK Postdoctoral fellowship.

References

1. Shipway A.N., Katz E. and Willner I., Nanoparticle Arrays on Surfaces for Electronic, Optical and Sensor Applications, *Chemphyschem*, **1**, 18-52 **(2000)**

2. McFarland A.D. and Duyne R.P.V., Single Silver Nanoparticles as Real-Time Optical Sensors with Zeptomole Sensitivity, *Nano Lett.*, **3**, 1057-1062 **(2003)**

3. Nath N. and Chilkoti A.A., Colorimetric Gold Nanoparticle Sensor to Interrogate Biomolecular Interactions in Real Time on a Surface, *Anal. Chem.*, **74**, 504–509 **(2002)**

4. Jain P.K., Huang X., Ivan H., Sayed EI. and Sayed M.A., Noble Metals on the Nanoscale: Optical and Photothermal Properties and Some Applications in Imaging, Sensing, Biology and Medicine, *Acc. Chem. Res.*, **41**, 1578–1586 **(2008)**

5. Gatzen H.H. and Leuthold V.S.J., Doping and Surface Modification, Springer **(2015)**

6. Cui Z., Nanofabrication, Springer **(2008)**

7. Whitesides G.M. and Grzybowski B., Self-assembly at all scales, *Science*, **295**, 2418-2121 **(2002)**

8. Baruwati B., Polshettiwar V. and Varma R.S., Glutathione Promoted Expeditious Green Synthesis of Silver Nanoparticles in Water Using Microwaves, *Green Chem.*, **11**, 926-930 **(2009)**

9. Grzelczak M., Vermant J., Furst E.M. and Liz-Marzán L.M., Directed Self-Assembly of Nanoparticles, *ACS Nano*, **4**, 3591-3605 **(2010)**

10. Khamarui S., Saima Y., Laha R.M., Ghosh S. and Maiti D.K., *Sci. Rep.*, **5**, 8636-8641 **(2015)**

11. Ikkala O. and Brinke G.T., Functional Materials Based on Self-assembly of Polymeric Supramolecules, *Science*, **295**, 2407-2409 **(2002)**

12. Busseron E., Ruff Y., Moulin E. and Giuseppone N., Supramolecular Self-assemblies as Functional Nanomaterials, *Nanoscale*, **5**, 7098-7140 **(2013)**

13. Kim C.K., Kalluru R.R., Sing J.P., Fortner A., Griffin J., Darbha G.K. and Ray P.C., Gold-nanoparticle-based Miniaturized Laser-induced Fluorescence Probe for Specific DNA Hybridization Detection: Studies on Size-dependent Optical Properties, *Nanotech*, **17**, 3085-3093 **(2006)**

14. Jansa H. and Huo Q., Gold Nanoparticle-enabled Biological and Chemical Detection and Analysis, *Chem. Soc. Rev.*, **41**, 2849-2866 **(2012)**

15. Kreibig U. and Vollmer M., Optical Properties of Metal Clusters, Springer-Verlag, Berlin **(1995)**

16. Shipway A.N., Katz E. and Willner I., Nanoparticle Arrays on Surfaces for Electronic, Optical and Sensor Applications, *Chem Phys Chem.*, **1**, 18-52 **(2000)**

17. Hu L., Chen M., Fang X. and Wu L., Oil–water Interfacial Self-assembly: a Novel Strategy for Nanofilm and Nanodevice Fabrication, *Chem. Soc. Rev.*, **41**, 1350-1362 **(2012)**

18. Storhoff J.J., Elghanian R., Mucic R.C., Mirkin C.A. and Letsinger R.L., One-Pot Colorimetric Differentiation of Polynucleotides with Single Base Imperfections Using Gold Nanoparticle Probes, *J. Am. Chem. Soc.*, **120**, 1959-1964 **(1998)**

19. Dutta T. and Sarkar S., Nanocarbon–{[Na10(PrW10O36)] 2·130H2O} composite to detect toxic food coloring dyes at nanolevel, *Appl. Nanosci.*, DOI 10.1007/s13204-016-0529-8 **(2016)**

20. Narayanan R. and El-Sayed M.A., Catalysis with Transition Metal Nanoparticles in Colloidal Solution: Nanoparticle Shape Dependence and Stability, *J. Phys. Chem. B*, **109**, 12663-12676 **(2005)**

21. Polshettiwar V. and Varma R.S., Green Chemistry by Nano-catalysis, *Green Chem.*, **12**, 743-754 **(2010)**

22. Gayen K.S., Sengupta T., Saima Y., Das A., Maiti D.K. and Mitra A., Cu (0) Nanoparticle Catalyzed Efficient Reductive Cleavage of Isoxazoline, Carbonyl Azide and Domino Cyclization in Water Medium, *Green Chem.*, **14**, 1589-1592 **(2012)**

23. Ahammed S., Kundu D. and Ranu B.C., Cu-Catalyzed Fe-Driven C_{sp}–C_{sp} and C_{sp}–C_{sp2} Cross-Coupling: An Access to 1,3-Diynes and 1,3-Enynes, *J. Org. Chem.*, **79**, 7391-7398 **(2014)**

24. Hassenkam T., Moth-Poulsen K., Stuhr-Hansen N., Orgaard K., Kabir M.S. and Bjornholm T., Self-Assembly and Conductive Properties of Molecularly Linked Gold Nanowires, *Nano Lett.*, **4**, 19-22 **(2004)**

25. Reda S.M. and Al-Ghannam S.M., Synthesis and Electrical Properties of Polyaniline Composite with Silver Nanoparticles, *Adv. Mater. Phys. Chem.*, **2**, 75-81 **(2012)**

26. Pelka J.B., Brust M., Gierlowski P., Paszkowicz W. and Schell N., *Appl. Phys. Lett.*, **89**, 063110-063115 **(2006)**

27. Steinecker S.H., Rowe M.P. and Zellers E.T., Model of Vapor-Induced Resistivity Changes in Gold−Thiolate Monolayer-Protected Nanoparticle Sensor Films, *Anal. Chem.*, **79**, 4977-4986 **(2007)**

28. Joseph Y., Peic A., Chen X., Michl J., Vossmeyer T. and Yasuda, Vapor Sensitivity of Networked Gold Nanoparticle Chemiresistors: Importance of Flexibility and Resistivity of the Interlinkage, *J. Phys. Chem. C*, **111**, 12855-12859 **(2007)**

29. Shumaila G.B., Lakshmi V.S., Alam M., Siddiqui A., Zulfequar M.M. and Husain M., Synthesis and Characterization of Se Doped Polyaniline, *Curr. Appl. Phys.*, **11**, 217-222 **(2010)**

30. Prateek, Thakur V.K. and Gupta R.K., Recent Progress on Ferroelectric Polymer-Based Nanocomposites for High Energy

Density Capacitors: Synthesis, Dielectric Properties and Future Aspects, *Chem. Rev.*, **116**, 4260-4317 **(2016)**

31. Shan J. and Tenhu H., Recent Advances in Polymer Protected Gold Nanoparticles: Synthesis, Properties and Applications, *Chem. Commun.*, DOI: 10.1039/B707740H, 4580-4598 **(2007)**

32. Ray S., Das A.K. and Banerjee A., Smart Oligopeptide Gels: *in situ* Formation and Stabilization of Gold and Silver Nanoparticles within Supramolecular Organogel Networks, *Chem. Commun.*, DOI: 10.1039/B605498F, 2816-2818 **(2006)**

33. Palui G., Ray S. and Banerjee A., Synthesis of Multiple Shaped Gold Nanoparticles Using Wet Chemical Method by Different Dendritic Peptides at Room Temperature, *J. Mat. Chem*., **19**, 3457-3468 **(2009)**

34. Si S. and Mandal T.K., Tryptophan-based Peptides to Synthesize Gold and Silver Nanoparticles: A Mechanistic and Kinetic Study, *Chem. Eur. J.*, **13**, 3160-3168 **(2007)**

35. Graf P., Mantion A., Foelske A., Shkilnyy A., Masic A. and Thünemann A.F., Peptide-Coated Silver Nanoparticles: Synthesis, Surface Chemistry and pH-Triggered, Reversible Assembly into Particle Assemblies, *Chem Eur J*, **15**, 5831-5835 **(2009)**

36. Wagner S.C., Roskamp M., C¨olfen H., B¨ottcher C., Schlecht S. and Koksch B., Switchable Electrostatic Interactions Between Gold Nanoparticles and Coiled Coil Peptides Direct Colloid Assembly, *Org. Biomol. Chem.*, **7**, 46-51 **(2009)**

37. Chatterjee N., Pandit P., Halder S., Patra A. and Maiti D.K., Generation of Nitrile Oxides under Nanometer Micelles Built in Neutral Aqueous Media: Synthesis of Novel Glycal-Based Chiral Synthons and Optically Pure 2, 8-Dioxabicyclo [4.4.0] decene Core, *J. Org. Chem.*, **73**, 7775-7778 **(2008)**

38. Maiti D.K., Halder S., Pandit P., Chatterjee N., De D., Joarder D., Pramanik N., Saima Y., Patra A. and Maiti P.K., Synthesis of Glycal-Based Chiral Benzimidazoles by $VO(acac)_2$−$CeCl_3$Combo Catalyst and Their Self-Aggregated Nanostructured Materials, *J. Org. Chem.*, **74**, 8086-8097 **(2009)**

39. Maiti, D.K., Chatterjee N., Pandit P. and Hota S.K., Generation of Azomethine imine and Metal-free Formal 1,3-dipolar Cycloaddition of Imine with PhIO: Reaction, Scope and Synthesis, *Chem. Commun.*, **46**, 2022-2024 **(2010)**

40. Khamarui S., Maiti R. and Maiti D.K., Reactant Cum Solvent Water: Generation of Transient λ^3-Hypervalent Iodine, Its Reactivity, Mechanism and Broad Application, *RSC Advances*, **5**, 106633-106643 **(2015)**

41. Frisch M.J. et al, Gaussian 09, Revision D.01, Gaussian, Inc., Wallingford CT **(2009)**

42. Pelka J.B., Brust M., Gierlowski P., Paszkowicz W. and Schell N., *Appl. Phys. Lett.*, **89**, 063110 **(2006)**.

(Received 10th September 2017, accepted 05th November 2017)